

Resonant magnetic excitations at high energy in superconducting $\text{YBa}_2\text{Cu}_3\text{O}_{6.85}$

S. Pailhès¹, Y. Sidis¹, P. Bourges^{1*}, V. Hinkov², A. Ivanov³, C. Ulrich², L.P. Regnault⁴ and B. Keimer²

¹ *Laboratoire Léon Brillouin, CEA-CNRS, CE-Saclay, 91191 Gif sur Yvette, France.*

² *Max-Planck-Institut für Festkörperforschung, 70569 Stuttgart, Germany*

³ *Institut Laue Langevin, 156X, 38042 Grenoble cedex 9, France.*

⁴ *CEA Grenoble, DRFMC, 38054 Grenoble cedex 9, France.*

A detailed inelastic neutron scattering study of the high temperature superconductor $\text{YBa}_2\text{Cu}_3\text{O}_{6.85}$ provides evidence of new resonant magnetic features, in addition to the well known resonant mode at 41 meV: (i) a commensurate magnetic resonance peak at 53 meV with an even symmetry under exchange of two adjacent CuO_2 layers; and (ii) high energy incommensurate resonant spin excitations whose spectral weight is around 54 meV. The locus and the spectral weight of these modes can be understood by considering the momentum shape of the electron-hole spin-flip continuum of d -wave superconductors. This provides new insight into the interplay between collective spin excitations and the continuum of electron-hole excitations.

The spin excitation spectrum of the copper oxide superconductors is modified markedly upon entering the superconducting state. In materials with transition temperatures, T_c , exceeding about 50 K, a “resonant mode” emerges below T_c around the wavevector $\mathbf{Q}_{\text{AF}} \equiv (\pi/a, \pi/a)$ characteristic of antiferromagnetism (AF) in the undoped parent compounds[1]. Materials in which the mode has been observed include cuprates with one $\text{Ti}_2\text{Ba}_2\text{CuO}_{6+\delta}$ ($\text{Ti}2201$) [2] and two ($\text{YBa}_2\text{Cu}_3\text{O}_{6+x}$ [3, 4, 5], $\text{Bi}_2\text{Sr}_2\text{CaCu}_2\text{O}_{8+\delta}$ [6]) CuO_2 planes per unit cell. Very recently, an analogous feature has been observed in the single-layer material $\text{La}_{2-x}\text{Ba}_x\text{CuO}_4$ as well, but details of its temperature dependence are not yet known [7]. The results of angle resolved photoemission spectroscopy (ARPES) [8], optical conductivity [9], and tunneling [10] experiments on $\text{Bi}_2\text{Sr}_2\text{CaCu}_2\text{O}_{8+\delta}$ have been interpreted as evidence of strong interactions of charged quasiparticles with this magnetic mode. The mode therefore plays a prominent role in current theories of high temperature superconductivity [11, 12]. Most models proposed to explain the resonant mode are based on strong electronic correlations [11, 12, 13, 14, 15, 16, 17, 18, 19, 20, 21, 22, 23, 24]. In an itinerant-magnetism picture, the mode is assigned to an excitonic bound state in the superconductivity-induced gap in the spectrum of electron-hole spin-flip excitations [11, 12, 13, 14, 15, 16, 17, 18]. In local-moment models, the mode is viewed as a magnon-like excitation characteristic of a magnetically ordered phase competing with the superconducting state [19, 20, 21, 22, 23, 24].

Early experiments on the resonant [3] mode were focused on the wavevector \mathbf{Q}_{AF} , where its spectral weight is maximum. Recent advances in neutron scattering instrumentation have made it possible to resolve weaker features of the spin excitations, which further constrain the theoretical description of the mode and its interaction with charged quasiparticles. First, incommensurate excitation branches both below and above 41 meV[25, 26] were found to merge at \mathbf{Q}_{AF} , forming continuous dispersion relations with an X-shape. In addition a sec-

ond, disconnected mode was recently observed in slightly overdoped $\text{Y}_{0.9}\text{Ca}_{0.1}\text{Ba}_2\text{Cu}_3\text{O}_7$ ($T_c=85$ K) [27]. Two magnetic modes with odd and even symmetry with respect to exchange of two adjacent CuO_2 layers are expected on general grounds in a bilayer material such as $(\text{Y}, \text{Ca})\text{Ba}_2\text{Cu}_3\text{O}_7$. In the overdoped material, the odd and even modes were observed at 36 and 43 meV, respectively. The energy difference is in good agreement with the interlayer exchange interaction, $J_{\perp} \sim 10$ meV, extracted from the spin wave dispersions in antiferromagnetically ordered $\text{YBa}_2\text{Cu}_3\text{O}_{6.15}$ [28].

In slightly underdoped $\text{YBa}_2\text{Cu}_3\text{O}_{6.85}$, only the odd mode has thus far been observed at an energy of 41 meV. A survey of the high energy spectrum has now revealed a weak, even counterpart at 53 meV. While the even mode was expected to be present on general grounds, the survey has also uncovered an unexpected incommensurate excitation branch separated from both of these modes by a “silent band”, where spin excitations are not observed. The presence of silent bands in the spectrum of collective spin excitations can be understood by considering the momentum shape of the Stoner continuum of spin-flip excitations in a d -wave superconductor.

The experiment was performed on the same sample used in Ref. [25], and the measurements were taken at the recently upgraded IN8 triple axis spectrometer at the Institute Laue Langevin (Grenoble, France). The IN8 beam optics include vertically and horizontally focusing monochromator and analyzer, corresponding of arrays of Cu (200) crystals and pyrolytic graphite (002) crystals, respectively. The measurements were performed with a fixed final neutron energy of 35 meV. A filter was inserted into the scattered beam in order to eliminate higher order contamination. The crystal was oriented such that momentum transfers \mathbf{Q} of the form $\mathbf{Q} = (H, H, L)$ were accessible. We use a notation in which \mathbf{Q} is indexed in units of the tetragonal reciprocal lattice vectors $2\pi/a = 1.64\text{\AA}^{-1}$ and $2\pi/c = 0.54\text{\AA}^{-1}$. Excitations of even (e) and odd (o) symmetry can be identified by virtue of their magnetic structure factors along the c -direction.

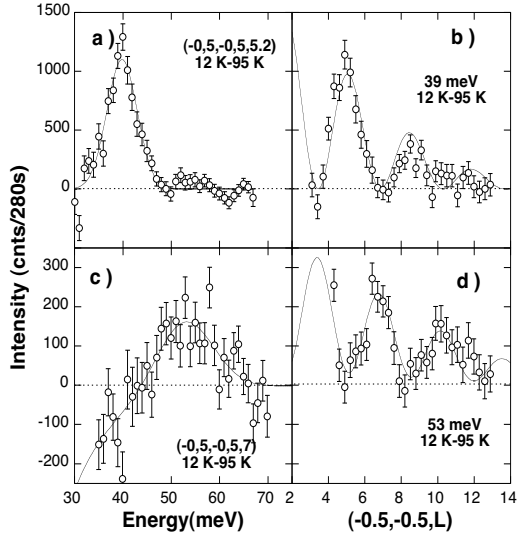


FIG. 1: Differences between energy scans measured at 12 K ($< T_c$) and 95 K ($> T_c$): a) in the odd channel at $(-0.5, -0.5, 5.2)$, c) in the even channel at $(-0.5, -0.5, 7)$. Differences between 10K and 95K of constant energy scan along the (001) direction: b) at 39 meV, d) at 53 meV. The lines in b) follow the sine-square modulation and in d) the cosine-square modulation of Eq. 1 convolved by the spectrometer resolution function.

As discussed in Ref. [27], the neutron scattering cross section can be written as,

$$\frac{\partial^2 \sigma(\mathbf{Q}, \omega)}{\partial \Omega \partial \omega} \propto f^2(Q) \left[\sin^2(\pi z L) \text{Im}[\chi_o(\mathbf{Q}, \omega)] + \cos^2(\pi z L) \text{Im}[\chi_e(\mathbf{Q}, \omega)] \right], \quad (1)$$

where $z c = 3.3 \text{ \AA}$ is the distance between CuO_2 planes within a bilayer unit, and $f(Q)$ is the magnetic form factor of Cu^{2+} .

Fig. 1a shows the difference between constant- \mathbf{Q} scans measured at 12 K ($< T_c$) and 95 K ($> T_c$) and at the wave vector $(-0.5, -0.5, 5.2)$ [29]. The enhancement of the scattering intensity at $E_r^o = 41 \text{ meV}$ below T_c heralds the well know resonance peak in the odd channel. Constant-energy scans at 39 meV indicate that the resonant excitation is centered at \mathbf{Q}_{AF} (Fig. 2a) and display the expected $[f^2(Q) \sin^2(\pi z L)]$ modulation along c^* (Fig. 1b). Since the dispersion of the odd mode has been well documented, it was not studied in detail, but constant-energy and constant- \mathbf{Q} profiles with excitation energies around E_r^o (Figs. 1 and 2) are in good agreement with the dispersion relations [30] described in Refs. [25, 26]. In particular, the asymmetric lineshape of the constant-energy cut at 45 meV (Fig. 1a) can be reproduced by assuming an upward dispersion similar to that reported for $\text{YBa}_2\text{Cu}_3\text{O}_{6.95}$ [26]. The asymmetry is due to a standard resolution focusing effect.

In addition to the odd resonance, we discovered a

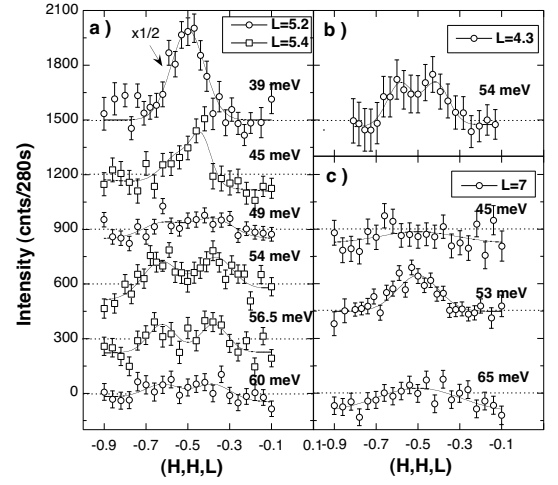


FIG. 2: Differences between 12 K ($< T_c$) and 95 K ($> T_c$) of constant energy scans measured along the (110) direction around $(-0.5, -0.5, L)$: a) $L=5.2$ or 5.4 (odd channel), b) $L=7$ (even channel), c) $L=4.3$ (mixed channel). For the sake of clarity, scans are shifted by 300 counts with decreasing energy from bottom to top.

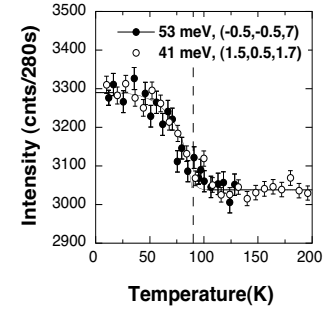


FIG. 3: (full circles) Temperature dependence of the neutron intensity at $\mathbf{Q}_{AF} = (0.5, 0.5, 7)$ at the even mode energy $E_r^e = 53 \text{ meV}$. The intensity has been scaled at 12 K and 125 K to that of the odd mode at 41 meV (open circles), measured under different experimental conditions [25].

second resonant magnetic excitation at higher energy. At $\mathbf{Q}_{AF} = (-0.5, -0.5, 7)$, where the structure factor for even excitations is maximum, an enhancement of the response in the superconducting state occurs at $E_r^e = 53 \text{ meV}$ (Fig. 1c). At this energy, the signal is peaked at the AF wave vector (Fig. 2c). Since its amplitude decreases with increasing \mathbf{Q} following the magnetic form factor, it can be identified as magnetic (Fig. 1d). Furthermore, its $[f^2(Q) \cos^2(\pi z L)]$ modulation along c^* demonstrates that it has an even symmetry (Fig. 1d). Finally, the signal decreases precipitously at T_c , as observed for the magnetic resonance in the odd channel (Fig. 3).

Even and odd resonance peaks also exhibit significant differences. First, the enhancement of the magnetic response in the superconducting state is six times weaker at E_r^e than at E_r^o . This explains why the even mode could not be observed in prior experiments with weaker neutron

flux. Second, both the constant-energy and the constant- Q profiles of the even spin excitation are broader than those of the odd mode. Gaussian fits of constant-energy scans provide an intrinsic full-width-at-half-maximum (FWHM) of $\Delta Q = 0.41 \pm 0.05 \text{ \AA}^{-1}$ at 53 meV in the even channel (Fig. 2c) whereas $\Delta Q = 0.25 \pm 0.05 \text{ \AA}^{-1}$ at 39 meV in the odd channel (Fig. 2a). In energy, the even resonance peak displays an intrinsic FWHM of 11 meV, in contrast to the resolution-limited odd mode. We performed a series of constant-energy scans in the even channel at energies above and below E_r^e , but could not resolve a dispersion analogous to that of the odd mode. We note, however, that the energy and wave vector resolutions at 53 meV are significantly broader than at 41 meV. Further study is required to ascertain whether the comparatively large energy and Q -widths of the even profiles are due to an intrinsic damping of the mode, or due to an unresolved dispersion relation. Leaving these details aside, it is interesting to note that the energies of even and odd resonance peaks deviate by ± 6 meV from 47 meV, the resonance peak energy of the mono-layer system $\text{Tl}_2\text{Ba}_2\text{CuO}_{6+\delta}$ [2] at optimal doping. This splitting can be understood as a consequence of the interlayer AF exchange coupling within a bilayer unit, which is known to be of similar magnitude ($J_\perp \sim 10$ meV).

Surprisingly, the survey of the magnetic spectrum in the energy range 50-60 meV has uncovered another set of excitations (Fig. 2a) distinct from the commensurate even mode. Constant-energy scans show clear symmetric incommensurate magnetic excitations at $\mathbf{Q}_{\text{IC}} = (-0.5 \pm \delta, -0.5 \pm \delta, L)$ with $\delta = 0.12$ r.l.u both in the odd channel at $L = 5.4$ (Fig. 2a) and in the mixed channel at $L = 4.3$ (Fig. 2a). The temperature dependence of the IC peak intensity at $\mathbf{Q}_{\text{IC}} = (-0.62, -0.62, 5.4)$ and 54 meV displays a marked decrease when the temperature is raised above T_c (Fig. 4.a), as previously reported for both odd and

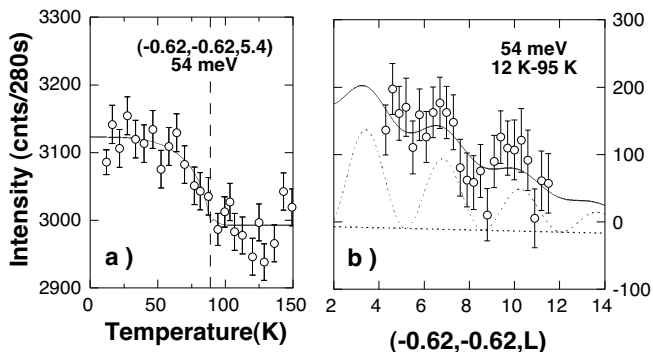


FIG. 4: Temperature dependence of the neutron intensity at the odd wave vector $(-0.62, -0.62, 5.4)$ and at $E = 54$ meV. b) Difference between constant energy scans at 12 K and 95 K along the (001) direction. The full line is a fit of the data by a combination of the odd and even modulations (see text). For clarity, the contribution from the commensurate even resonant mode is represented by the dashed line.

even resonance peaks (Fig. 3). In addition, the IC peak intensity decreases along c^* following $f^2(Q)$, as expected for a magnetic signal (Fig. 4b). It is not straightforward to deduce the symmetry of the IC resonant excitations from the L -dependence measured at \mathbf{Q}_{IC} , because it overlaps with the cosine-square modulation of the nearby even resonance peak. To overcome this difficulty, we fitted all of the data around 53-54 meV reported in Figs. 1d, 2a-c, and 4b simultaneously, assuming an L -dependence for the IC spin excitation of the form $[f^2(Q)(\gamma \sin^2(\pi z l) + (1 - \gamma) \cos^2(\pi z l))]$. The best fit is given by $\gamma = 0.8 \pm 0.15$, which means that these incommensurate excitations exhibit predominantly an odd symmetry. The intensity of the IC spin fluctuations passes through a maximum around 54 meV, where it reaches about 1/7 of the odd resonance intensity (Fig. 2a). In the energy range from ~ 50 meV to ~ 60 meV, the position of the IC peaks, $\delta \simeq 0.12$ r.l.u., is energy independent within the error and the IC peaks are symmetric on both sides of \mathbf{Q}_{AF} , in contrast to the resolution focusing effect observed at 45 meV (Fig. 2a). Interestingly, the IC intensity drops around 49 meV separating both behaviors (Fig. 2a).

Fig. 5a provides a synopsis of all spin excitation branches revealed in this study. The figure suggests that the high energy IC excitation branch is a continuation of the upper dispersion branch emanating from the odd resonance at 41 meV. However, the data of Fig. 2 demonstrate that the intensity along this branch is dramatically reduced around 49 meV and $\delta \sim 0.1 - 0.11$. This “dark region” is marked by the hatched area in Fig. 5a. It had been noticed before that the lower excitation branch emanating from 41 meV also fades out rapidly as it approaches $\delta \sim 0.1$ [25]. Interestingly, therefore, the spin fluctuation intensity is very weak in a narrow “silent band” around $\delta \sim 0.1 - 0.11$ over the entire energy range (Fig. 5a).

We will argue now that the presence of “silent bands”, the upper cutoff of the IC spin excitations, and the intensity ratio of odd and even modes can be understood by considering the shape of the electron-hole spin flip continuum of a d -wave superconductor. To illustrate this point, Fig. 5c displays the SC d -wave continuum along the (110) direction for the Fermi surface shown in Fig. 5b. Realistic calculations show that collective modes within the continuum or the continuum itself is likely much too weak to be directly observed by inelastic neutron scattering experiments. Therefore, only collective modes located below the e - h continuum can actually be detected. The continuum threshold exhibits a steep minimum in the vicinity of the wave vector $2\mathbf{k}_N$ corresponding to scattering between nodes of the d -wave gap function (Fig. 5b). This provides a natural explanation for the “silent bands” of Fig. 5a.

In the same picture, the high energy IC excitations can be understood as collective modes in zone II of the gap in the electron-hole spin-flip continuum, whereas the odd

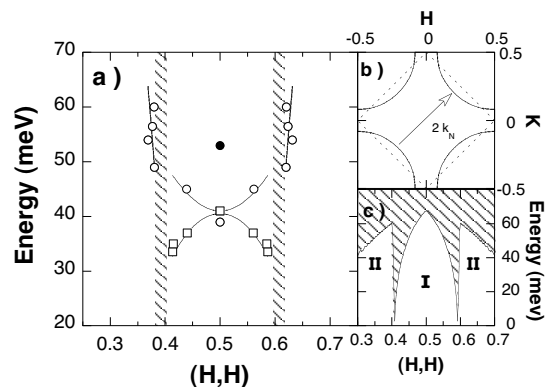


FIG. 5: a) Energy distribution of the resonant spin excitations along the (110) direction: open (full) circles stand for excitation with odd (even) symmetry (from Fig. 2). The downward dispersion observed in [25] is reproduced, assuming it is isotropic (open squares). The vertical hatched areas indicate the locus of the “silent band” described in the text. b) Typical Fermi surface measured by ARPES in BSCO [13, 31]. c) Electron-hole spin-flip continuum along the (110) direction of a d -wave superconductor with a maximum superconducting gap of 35 meV. The continuum goes to zero energy for $2\mathbf{k}_N = (0.5 \pm \delta, 0.5 \pm \delta)$ with $\delta \simeq 0.11$ r.l.u. joining the nodal points at the Fermi surface (arrow in b).

and even excitation branches emanating from \mathbf{Q}_{AF} are collective states in zone I. The upper cutoff of the IC excitation branch can then be identified with the energy threshold, $\hbar\omega_c$, of the continuum in zone II. An upper cutoff of 60 meV is well reproduced by assuming a maximum superconducting gap of 35 meV (Fig.5c), consistent with the gap values extracted from ARPES and Raman scattering measurements around optimum doping. As discussed in Refs. 16, 27, an independent estimate of the continuum threshold in zone I can be obtained through the intensity ratio of the odd and even modes at \mathbf{Q}_{AF} . In theories according to which the resonant spin excitations correspond to collective $S=1$ modes pulled below the continuum by antiferromagnetic interactions, the spectral weights of the resonant modes are approximately proportional to their binding energies, $\hbar\omega_c - E_r^e$ and $\hbar\omega_c - E_r^o$. Depending whether energy-integrated intensities or peak intensities are compared, the spectral weight ratio is either 3 or 6, yielding $\hbar\omega_c = 66$ meV and 55 meV, respectively. Fig. 5c shows that the estimate $\hbar\omega_c$ obtained in this way is in good agreement with that from the high-energy IC excitations discussed above.

In conclusion, our inelastic neutron scattering experiment in $\text{YBa}_2\text{Cu}_3\text{O}_{6.85}$ has uncovered a commensurate magnetic resonance peak of even symmetry at 53 meV; its intensity is 6 times weaker than the well-known odd mode at 41 meV. Further, we have found high-energy spin excitations with a weakly energy-dependent incommensurability, separated by a “silent band” from the 41 meV mode. The silent band and other features of the spin exci-

tation spectrum can be understood as fingerprints of the interaction of collective spin excitations with electron-hole excitations. They can thus be regarded as counterparts of the self-energy effects of charged quasiparticles revealed in various spectroscopies [8, 9, 10, 11, 12]. A quantitative description of the excitation spectrum of Fig. 5a is a challenge for both itinerant and local-moment theories of magnetic excitations in the cuprates.

* To whom correspondence should be addressed; E-mail: bourges@bali.saclay.cea.fr

- [1] For a recent review: Y. Sidis *et al.*, cond-mat/0401328.
- [2] H.F. He *et al.*, Science **295**, 1045 (2002).
- [3] J. Rossat-Mignod *et al.*, Physica C **185-189**, 86 (1991); H.A. Mook *et al.*, Phys. Rev. Lett. **70**, 3490 (1993); H.F. Fong *et al.*, Phys. Rev. B **54**, 6708 (1996).
- [4] H.F. Fong *et al.*, Phys. Rev. B **61**, 14773 (2000).
- [5] P. Dai *et al.*, Phys. Rev. B **63**, 054525 (2001).
- [6] H.F. Fong *et al.*, Nature **398**, 588 (1999).
- [7] J.M. Tranquada *et al.*, cond-mat/0401621.
- [8] A. Kaminski *et al.*, Phys. Rev. Lett., **86**, 1070 (2001); P. Johnson *et al.*, Phys. Rev. Lett., **87**, 177007 (2001); S.V. Borisenko, *et al.*, Phys. Rev. Lett., **90**, 207001 (2003).
- [9] J.P. Carbotte, *et al.*, Nature, **401**, 304 (1999); J. Hwang, T. Timusk, G. D. Gu, Nature **427**, 714 (2004).
- [10] J.F. Zasadzinski, *et al.*, Phys. Rev. Lett. **87**, 067005 (2001), and references therein.
- [11] A. Abanov, *et al.* Phys. Rev. Lett. **89**, 177002 (2002).
- [12] M. Eschrig, M.R. Norman, Phys. Rev. Lett. **89**, 277005 (2002).
- [13] M. R. Norman Phys. Rev. B **63**, R092509 (2001).
- [14] D. van der Marel, Phys. Rev. B **51**, 1147 (1995).
- [15] D. Z. Liu, *et al.*, Phys. Rev. Lett. **75**, 4130 (1995).
- [16] A.J. Millis, H. Monien, Phys. Rev. B **54**, 16172 (1996).
- [17] F. Onufrieva, P. Pfeuty, Phys. Rev. B **65**, 054515 (2002).
- [18] I. Eremin, *et al.*, Phys. Rev. B **69**, (2004) (cond-mat/0309503).
- [19] D.K. Morr, D. Pines, Phys. Rev. Lett., **81**, 1086 (1998).
- [20] E. Demler, S.C. Zhang, Phys. Rev. Lett., **75**, 4126 (1995).
- [21] S. Sachdev *et al.*, Science **286**, 2479 (1999).
- [22] N. Hasselmann *et al.*, Phys. Rev. Lett. **82**, 2135 (1999).
- [23] C.D. Batista *et al.*, Phys. Rev. B **65**, 180402 (2002).
- [24] F. Krüger, S. Scheidl, Phys. Rev. B **67**, 134512 (2003); F. Krüger, S. Scheidl, cond-mat/0401354.
- [25] P. Bourges *et al.*, Science **288**, 1234 (2000).
- [26] D.Reznik *et al.*, cond-mat/0307591.
- [27] S. Pailhès *et al.*, Phys. Rev. Lett. **91**, 237002 (2003).
- [28] D. Reznik, *et al.*, Phys. Rev. B **53** R14741 (1996).
- [29] As previously reported [25], magnetic excitations, broad in both momentum and energy, are observed in the normal state in that sample. Following the standard technique, we perform a difference of the neutron intensity between ~ 12 K and ~ 100 K in order to identify the resonant enhancements of the spin susceptibility.
- [30] The downward (-) and upward (+) dispersions can be modeled by the relation: $E_{\pm} = \sqrt{(E_r^o)^2 \pm (\alpha_{\pm}q)^2}$ with $E_r = 40.5$ meV, $\alpha_- \simeq 125$ meV.Å and $\alpha_+ \simeq 110$ meV.Å.
- [31] A.A. Kordyuk, *et al.*, Phys. Rev. B **67**, R064504 (2003).